

See discussions, stats, and author profiles for this publication at: <https://www.researchgate.net/publication/257593379>

Pyrolytic Gasification of Post-consumer Polyolefins To Allow for "Clean" Premixed Combustion

DATASET *in* ENERGY & FUELS · JULY 2013

Impact Factor: 2.79 · DOI: 10.1021/ef4008592

CITATIONS

5

READS

51

5 AUTHORS, INCLUDING:



[Rasam Soheiliani](#)

Northeastern University

3 PUBLICATIONS 9 CITATIONS

SEE PROFILE



[Saber Talebi Anaraki](#)

Northeastern University

2 PUBLICATIONS 5 CITATIONS

SEE PROFILE



[Chuanwei Zhuo](#)

Cabot Corporation

24 PUBLICATIONS 139 CITATIONS

SEE PROFILE



[Yiannis Levendis](#)

Northeastern University

113 PUBLICATIONS 1,987 CITATIONS

SEE PROFILE

Pyrolytic Gasification of Post-consumer Polyolefins To Allow for "Clean" Premixed Combustion

Rasam Soheilian, Andrew Davies, Saber Talebi Anaraki, Chuanwei Zhuo, and Yiannis A. Levendis*

Department of Mechanical and Industrial Engineering, Northeastern University, Boston, Massachusetts 02115, United States

ABSTRACT: Utilization of post-consumer waste plastics as fuels is of technological interest because their energy contents (heating values) are comparable to those of premium fuels. Pyrolytic gasification of these solid polymers yields a mixture of predominately gaseous hydrocarbons and hydrogen. This gaseous fuel mixture can then be suitably blended with air and burned in well-controlled premixed flames. Such flames are much less polluting than diffusion flames, which would have been generated had the polymers been burned in their solid state. In this work, an apparatus was designed and built to continuously process polymers, in pelletized form, and to pyrolytically gasify them at temperatures in the range of 800–900 °C in N₂- or CO₂-containing environments. Subsequently, the gaseous pyrolyzates were mixed with air, ignited, and burned in a Bunsen-type burner in a manner similar to natural gas. Polyethylene and polypropylene pyrolyzates burned with blue-tint flames akin to those of natural gas. The flames were fairly steady and nearly stoichiometric, generating effluents with low CO/CO₂ ratios. The combustion reactions released heat in a small water boiler coupled to a miniature steam engine, which produced electricity, illustrating the feasibility of "clean" power generation from waste plastics. Because pyrolysis of polyolefins requires a nominal heat input that amounts to only a minuscule fraction of the heat released during their combustion, large-scale implementation of this technique is deemed to be technologically viable and economically favorable.

■ INTRODUCTION

Because their resources are finite, it is expected that fossil fuels will become scarce and costly at some point in the future. To ensure energy sustainability, it is thus imperative not only to improve the efficiency of energy use but also to identify and develop technologies for harnessing alternative energy sources. Readily available alternative fuels can be found in municipal/industrial recycling and waste streams. Nearly 5% of the yearly U.S. petroleum consumption is used to produce plastics, amounting to approximately 30 million tons.¹ In most applications, plastics are discarded upon use. A small fraction (7%) of the discarded plastics are recycled;² however, because plastics are degraded upon usage, there are limited markets for the recycled materials. In fact, most post-consumer plastics end up in landfills or generate ubiquitous litter. Because they are non-biodegradable, they generate a long-term solid waste issue. Direct combustion of post-consumer plastics in waste incinerators releases their stored internal energy (heating value), which is comparable to those of premium fuels.³ However, conventional direct combustion leads to diffusion flames, forming around the devolatilizing solid plastics (see Figure 1), which generate large amounts of health-hazardous soot, polycyclic aromatic hydrocarbons (PAHs), and other pollutants.

An alternative indirect combustion technique was followed in this work, which called for a two-step process: pyrolytic gasification of the solid polymers, followed by premixed combustion of the gaseous pyrolyzates with air. Such conditions afford effective mixing of gaseous fuel compounds with oxygen and can generate low emissions of pollutants.^{4–7} In fact, Goncalves et al.⁷ reported that indirect homogeneous combustion of polyethylene (PE) pyrolyzates released 10 times lower amounts of PAHs and particulates than direct

combustion of the same polymer, at similar furnace operating conditions.

Indirect combustion of the plastics (pyrolytic gasification followed by combustion of the pyrolyzate gases) is technically attractive, with Jinno et al.³ reporting values for the heat of pyrolysis of PE and the heat of pyrolysis of polypropylene (PP) that are well under 1 MJ/kg. Even after the higher temperatures encountered in pyrolytic gasification herein than those in the aforementioned work are taken into account, the heat of pyrolysis of polyolefins is in the range of 1.8–2.4 MJ/kg (see Appendix 1). When this value is compared to the heating values (energy contents) of polyolefins, which are in range of 44–46 MJ/kg, it becomes evident that only a small fraction of the heat released during combustion will be needed to be fed back to pyrolytically gasify them. Therefore, a gaseous fuel stream may be produced from waste polymeric feedstocks by implementing a heat integration, where only a small penalty in energy and, thus, in the operating cost of a power plant will be encountered in running the gasifier. On the basis of this principle, this study developed and tested a process that accepts post-consumer plastics and releases their internal energy through environmentally benign indirect combustion.^{4–7} The feasibility of this process has been proven using polyolefins, the most voluminous commercial plastics.

Polyolefins is the collective description for plastic types that include PE, low-density polyethylene (LDPE), linear low-density polyethylene (LLDPE), and high-density polyethylene (HDPE), and PP. Polyolefins are polymers produced from simple olefins (also called alkenes, with the general formula

Received: May 9, 2013

Revised: July 3, 2013

Published: July 5, 2013



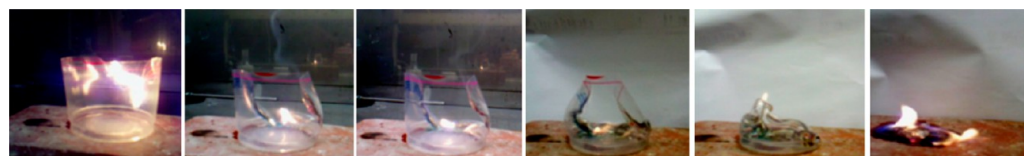


Figure 1. Direct combustion of post-consumer plastics generates acrid smoke containing both condensed-phase and gas-phase hazardous pollutants.

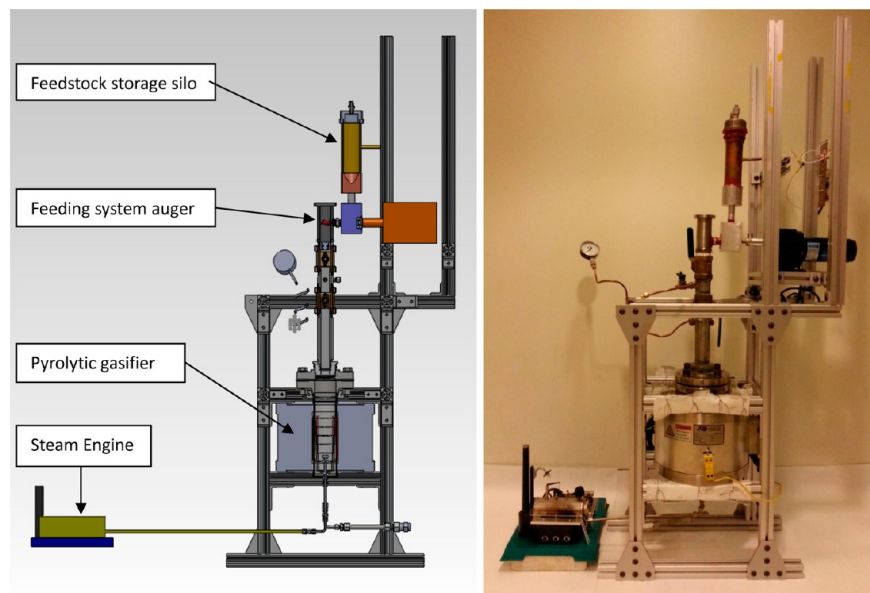


Figure 2. Laboratory-scale pyrolytic gasification apparatus designed and constructed for the needs of this study: (left) two-dimensional schematic detailing the apparatus architecture and (right) photograph of the actual system.

C_nH_{2n}) as monomers. Because of their versatility, low cost, inertness, and excellent chemical resistance, polyolefins are the most popular plastics in use today. Together they account for nearly half of Europe's total generation of 24 million tons and U.S.A.'s generation of 30 million tons of all plastics each year.¹

PE, either as high-density (HDPE) or low-density (LDPE), starts decomposing at 290 °C by scission of weak links and progressively by scission of tertiary carbon bonds or ordinary carbon bonds in the β position to tertiary carbons.⁸ Extensive weight loss is not observed until 370 °C is reached. The main products of its decomposition are an oil/wax product dominated by alkenes, alkynes, and alkadienes, a gas consisting mainly of alkanes and alkenes, and negligible char.^{4,9} The monomer precursor ethylene (ethene) is only one of many constituents of the volatile primary products. For instance, there is also formation of aromatic species, such as benzene and toluene. As the temperature of pyrolysis increases, gaseous products are favored. Extensive work by Conesa and co-workers¹⁰ examined the effects of the PE type, the effects of polymer branching, the effects of batch versus continuous operation, and the effects of the influence of the heating rate on the decomposition yields. They found variations in both the yields and the composition of the pyrolyzates, with branched PE yielding 91.8% gas with a higher aromatic content and less branched PE yielding 97.5% gas with lower aromatic content, both at 800 °C. These results are in good agreement with those by Scott et al.¹¹ and Kaminsky.¹² Westerhout et al.¹³ found that, at 800 °C, the product contains more methane than ethylene and low amounts of aromatics, and most importantly, they determined that the type of pyrolyzed PE, i.e., LDPE or HDPE, had no significant influence on the product spectrum produced.

The effect of the residence time and the temperature of pyrolysis on the product distribution was studied by Mastral et al.¹⁴ in two free-fall reactors, placed in series. Their experiments showed that, up to 700 °C, the main products obtained were waxes and oil fractions and that the gas yield increased as the temperature increased. The generation of aromatics was reported to be significant at 800 °C and showed an increasing trend with temperature and residence time. The main compounds present in the gas fraction were hydrogen, methane, and acetylene at temperatures up to 1000 °C. Longer residence times led to a more intense cracking of the aliphatic fractions, and the methane and ethylene yields increased significantly. Lee et al.¹⁵ reported on the oxidative gasification of mixed plastics in a 500 KW_{th} pilot-scale system, including a flame-assisted tar reformer and a sequential gas-cleaning process. The cleaned producer gas was composed mainly of hydrogen, carbon monoxide, carbon dioxide, and methane.

PP, having every other carbon in the main chain as a tertiary carbon, is prone to attack;⁸ this lowers the stability of PP compared to PE. PP starts decomposing at 230 °C by chain-scission and chain-transfer reactions;⁸ volatilization becomes significant above 300 °C.

High-temperature pyrolysis of PE and PP has been reported in the literature to generate a mix of light hydrocarbon gases, including methane, ethylene, propylene, butylene, etc.,^{13,14,16–21} and hydrogen.¹⁶

This experimental study aims at demonstrating that a high-energy-content gaseous fuel can be produced from post-consumer polyolefin feedstocks and can be burned in an environmentally benign manner, akin to natural gas, for power generation, process heat, or other energy-related applications. A

laboratory-scale system was designed and constructed to pyrolytically gasify pelletized polymers, at steady-state steady-flow conditions, and to generate a combustible gaseous fuel and burn it in a miniature steam engine to generate electricity. Pyrolytic gasification took place in both N_2 and CO_2 carrier gases. The reason for comparing these two background gases is because, whereas N_2 has to be purposely procured from a cryogenic air separation plant and is, thus, costly, a mixture of N_2 and CO_2 gases can be readily obtained at no cost by tapping to the exhaust effluent of a combustion system. In fact, this combustion system can burn the bulk of the gaseous fuel generated by the pyrolyzer. A slipstream of the effluent of the very same combustion process can be used to supply the pyrolyzer with a mixture of N_2 and CO_2 gases, upon removal of combustion-generated H_2O in a condenser. There may be other additional benefits to using CO_2 as the work by Yamada et al.²² has shown in the catalysis-aided reforming of the pyrolyzates of PE to CO and H_2 at 950 °C.

EXPERIMENTAL APPROACH

A laboratory-scale pyrolytic gasifier system has been designed and constructed to accept granulated plastics and, sequentially, liquefy and gasify them. The gaseous pyrolyzates are then mixed with air and burned in a nominally premixed burner. For demonstration purposes, the burner is also coupled with a miniature steam generator and steam engine setup to produce electricity (Wileco D18). The pyrolytic gasifier is shown in Figure 2. Its major components are a feedstock storing and feeding system and a heating chamber. The feeding system incorporates a reservoir with a hopper, where pelletized polymers are stored, an electric motor, and an auger/feeding box. Pellets are gravity-fed from the reservoir through the hopper. The variable-speed electric motor (Leeson Corp. model 985.613F, 8.7 N m peak torque, 0–94 rpm, continuous duty) drives the horizontally oriented auger, which carries the pellets from the feeding box to a vertical purge chamber, leading to the furnace. The rotating auger uses a sealed bearing to minimize leakage from the system and, thus, maintain the pressure of the inert carrier gas.

The furnace chamber is defined by a stainless-steel tube with a heated volume of nearly 3 L. This was sufficient to accommodate the expansion of the pyrolyzing polymers, which were fed with a mass feeding rate of 1 g/min, and the flow of the carrier gas, at an additional 1 L/min. The pressure buildup during these steady-state steady-flow experiments was only a very small fraction of an atmosphere. The furnace is heated by electrical resistance elements (ATS Series 3110), rated at 1.43 kW. The furnace is connected to a proportional–integral–derivative (PID) loop temperature controller (ATS Series XT16). This allows for precise and reliable regulation of the system temperature at any desired set point. The speed of the electric motor that drives the polymer-feeding system is adjusted to obtain the desired mass flow rate of plastic pellets. The direct-drive motor and screw-type auger system provide a linear relationship between the feeding rate and motor speed [revolutions per minute (rpm)].

Asymmetrically perforated disks have been inserted at several vertical locations in the tubular furnace to intercept the falling polymer pellets and facilitate their sequential melting and gasification. In this manner, the particles gasify in the radiation cavity of the furnace, instead of settling at its cooler bottom.

The gas exit tube in the chamber is elevated from the bottom, to prevent its plugging by settling tars, and it is protected by a conical roof to prevent impingement of any falling molten polymer ligaments. Furthermore, the system is fitted with two relief valves, rated at 234 kPa, to avoid overpressuring.

High-temperature gaskets (THERMA-PUR style 4122 corrugated metal gasket, manufactured by Garlock Sealing Technologies) were used for sealing the flanges. A typical centerline gas temperature distribution in the furnace, as measured by a type-K thermocouple (Omega), is shown in Figure 3, after correcting for radiation heat

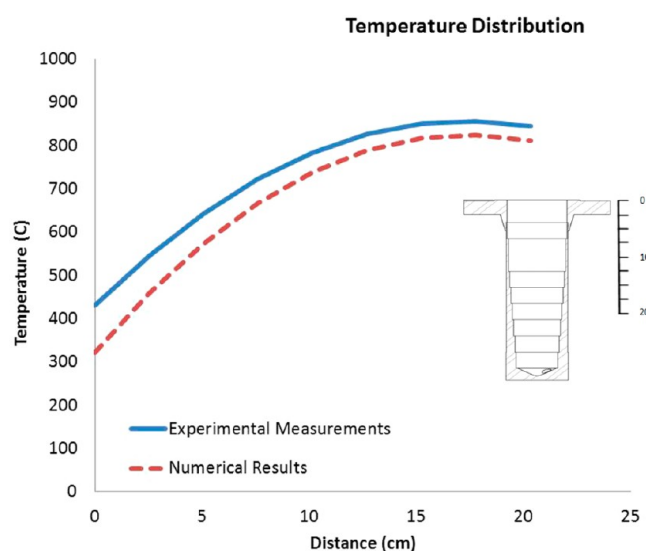


Figure 3. Comparison between experimental and numerical results of the gas temperature gradient at different elevations in the pyrolytic gasifier chamber, depicted in the inset, at a furnace set point of 950 °C.

transfer, as shown in Appendix 2. In this case, the controller was set to maintain a constant wall temperature of 950 °C. Temperature measurements were taken at each of the perforated disks in the chamber to gauge the uniformity of the heater. The temperature gradient plateaued in the bottom half of the chamber, where the maximum temperatures prevailed. Superimposed is also a temperature profile calculated by the numerical software ANSYS FLUENT, as outlined in a following section. The agreement is within 50 °C.

As mentioned before, it has been previously reported^{10,14,18,19} that the yield of gas from pyrolysis of PE increases with the temperature; it only accounts for 5.7 wt % at 500 °C, exceeds 90 wt % at $T_{\text{pyrolysis}} = 800$ °C, and slowly decreases thereafter with an increasing temperature. Therefore, a gas temperature of 800 °C was chosen in this work to maximize the yield of gaseous PE pyrolyzates while minimizing the generation of tars and oils. To account for heat losses throughout the system, the furnace controller set point was raised to the range of 900–950 °C to ensure reaching 800 °C in the pyrolysis chamber.

Characteristics of the Polyolefin Feedstocks. The two polyolefin polymer feedstock materials used in this study were LDPE with a chemical formula of $(C_2H_4)_n$ and PP with a chemical formula of $(C_3H_6)_n$. HDPE was not included in this study because it has been previously reported to decompose in a fashion similar to that of LDPE. Commercially available post-consumer plastics, in pelletized form, were obtained from a local supplier and used in these experiments (see Figure 4). LDPE has a density range of 0.91–0.94 g/cm³, whereas PP has a density range of 0.86–0.95 g/cm³.

Experimental Procedure. In each experiment, the pelletized polymers were loaded into the hopper and the feeding system was sealed. The carrier gas was N_2 or CO_2 at a flow rate of 1 L/min. These gases were used to purge the air out of the system and to ensure oxygen-free pyrolysis. Thereafter, the polymer pellets were introduced to the system at a targeted feeding rate. Typical plots of the feeding mass of pellets with time are shown in Figure 4. To obtain these data, the feeding system was detached from the pyrolysis apparatus and setup in a benchtop style experiment, with a calibrated mass balance (Mettler AE50) positioned to catch and measure the output. The hopper was loaded with plastic pellets, and the drive motor was run at a constant speed, with manual data readings taken every 5 s. The plots shown in Figure 4 demonstrate fairly linear overall rates of pellets in the broad neighborhood of 1 g/min.

In all subsequent experiments, the feeding rate of solid pelletized polymers in the furnace was set at 1 g/min based on experimentally determined repeatable steady-state operation of the feeder. This value also matched the capacities of two nominally premixed flame burners

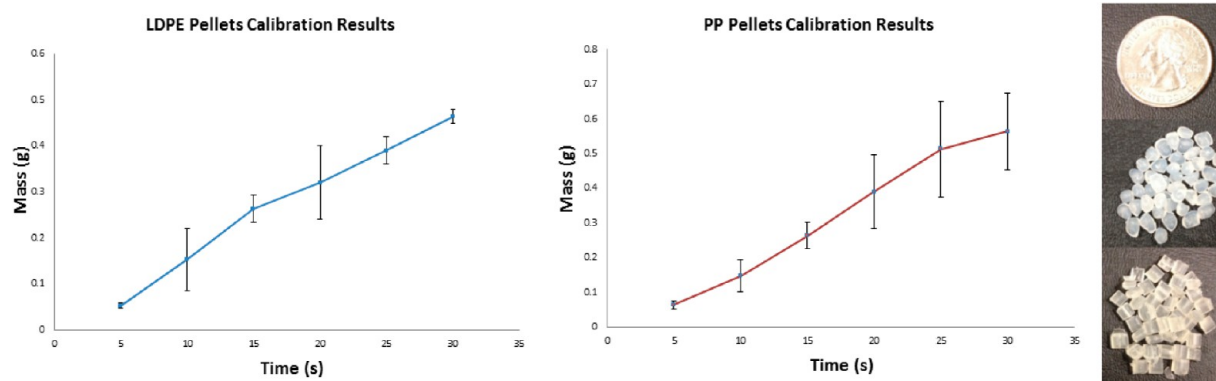


Figure 4. Feeding characteristics of (left) LDPE and (right) PP pellets used in this work. A total of 1 g quantities of (top) LDPE and (bottom) PP are depicted on the right.

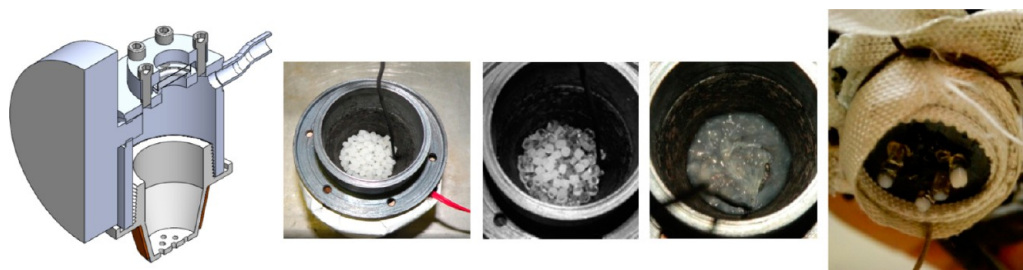


Figure 5. Demonstration of melting and dripping of polyolefins through the perforated plates used in the pyrolytic gasifier.²⁴ This experiment was conducted at lower temperatures than those encountered in the pyrolytic gasifier.

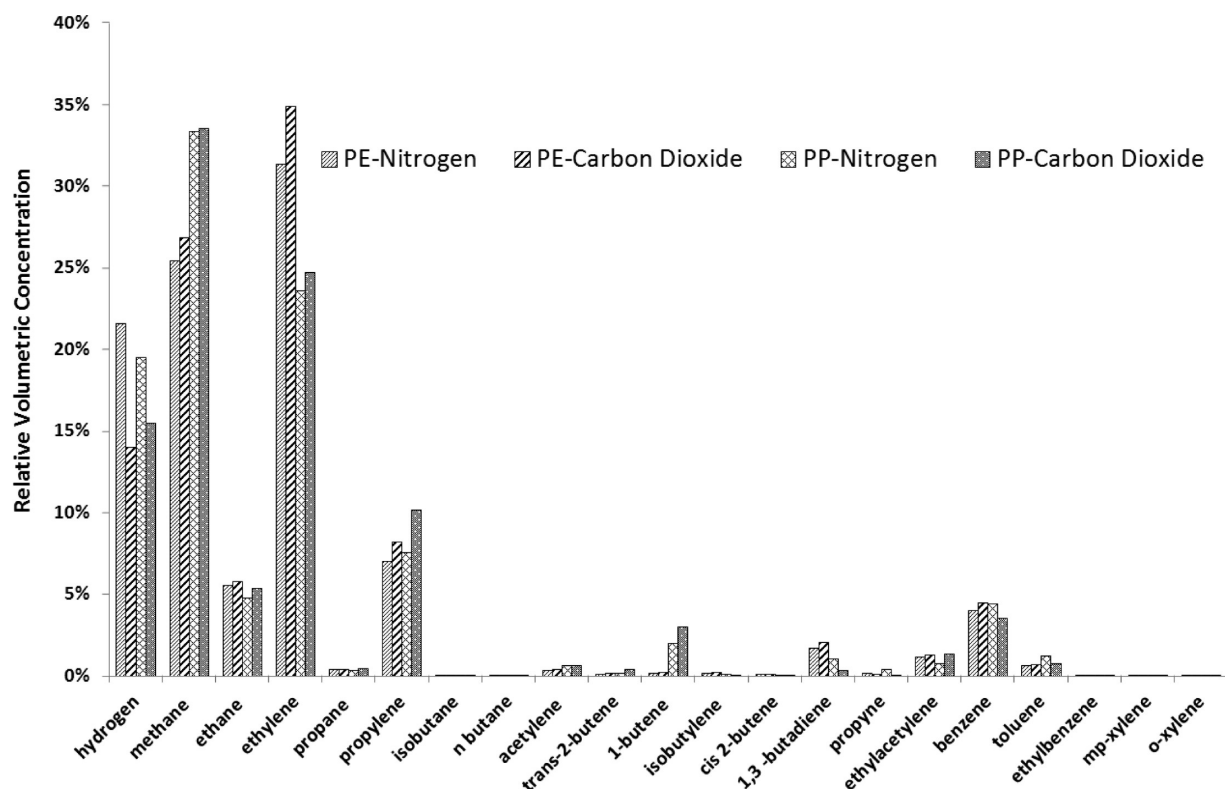


Figure 6. Composition of the effluent of pyrolytic gasification of PE and PP at 800 °C and a polymer heating rate of approximately 10 K/s.

used in this work: a Bunsen burner and a rectangular burner (measuring 2 × 14 cm), supplied with the miniature steam engine (Wileco D18). In this regard, the capabilities of both burners were tested using bottled ethylene gas (which has been identified as a major

pyrolyzate of the polyolefins). Because the ratio of the volume of the solid polymer to the volume of gaseous ethylene pyrolyzate is inversely proportional to the ratio of their respective densities (e.g., $\rho_{\text{solid PE}} = 940 \text{ kg/m}^3$, and $\rho_{\text{ethylene}} = 1.178 \text{ kg/m}^3$), the equivalent mass flow rate

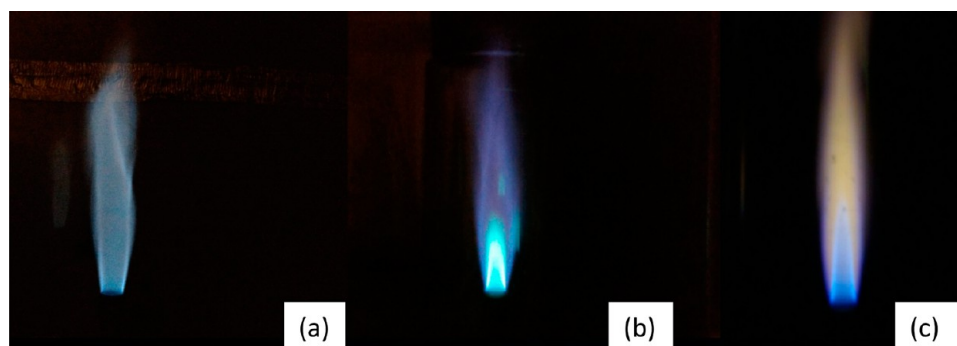


Figure 7. Nominally premixed flames of (a) natural gas, (b) PE pyrolyzate gases, and (c) PP pyrolyzate gases.

of ethylene gas to match the mass flow rate of the 1 g/min polymer pellets was determined to be 830 cm³/min. This flow rate of ethylene produced steady flames of appropriate intensity for the operation of the miniature engine.

Additional experiments were also conducted to explore the effect of the carrier gas (N₂) on the flammability and stability of the flames, with the motivation being that reduced inert gas flow rates are economically advantageous. Experiments were conducted at the aforementioned ethylene gas flow rate of 0.83 L/min and inert nitrogen flow rates varying by 3-fold. These findings of these experiments, in agreement with other pertinent findings elsewhere,²³ showed that the addition of various amounts of nitrogen inert gas did not significantly affect the flammability of the ethylene gas in the nominally premixed burners used herein.^{24,38}

The pyrolytic gasification chamber contained five perforated steel plates, placed at different axial locations in the furnace tube. The free-falling plastic pellets were intercepted by these plates and were heated, and as they melted, molten mass dripped through the plates, changing the state to liquid and then ultimately to gas. Subsequently, the effluent pyrolyzate gases (nominally 0.83 L/min) mixed with the carrier gas (1 L/min), then traveled through the exhaust pipe, and entered the burner.

A brief series of experiments was conducted to visualize the behavior of molten polymers through the perforated plates. To accomplish this, a quantity of pellets was placed in a stainless-steel crucible, whose bottom was perforated with several holes (see Figure 5). A thermocouple was placed in the fixed bed of particles to monitor the temperature. The crucible was then heated by an electric tape to temperatures approaching 300 °C. As the temperature of the bed increased, the plastic pellets softened, melted (at 250 °C), liquefied, and dripped through the holes. Because these experiments were conducted under a fume hood at standard temperature and pressure (STP) conditions, the dripping resolidified. However, inside the hot environment of the pyrolytic gasifier, it is expected that the drippings gasify.

NUMERICAL APPROACH

A two-dimensional (2D) model has been developed to assess the gas velocity profile and gas temperature distribution in the furnace using ANSYS FLUENT. On the basis of the velocity profile, a residence time of the pyrolyzates in the heated zone of the furnace was estimated with the assumption that the pellets were intercepted by the perforated plates, melted, and devolatilized therein. The k - ϵ model was used for simulating the velocity profile. In this simulation, nitrogen was used as the carrier gas at a flow rate of 1 L/min and, in a simplification, the pyrolyzate gases were considered to consist only of one compound, ethylene, which is a major component of polyolefin decomposition. The mass flow rate of ethylene was set at 0.83 L/min. The temperature distribution in the furnace was solved on the basis of the discrete transfer radiation model (DTRM), and it was assumed that the source of radiation was the hot wall

of the tubular furnace, which was maintained at a temperature of 950 °C (1223 K).

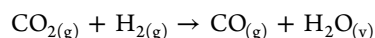
RESULTS AND DISCUSSION

Typical compositions of the pyrolyzates of PE and PP obtained herein are listed in Figure 6, when nitrogen and carbon dioxide were used as carrier gases. Chemical speciation was conducted with gas chromatography, using a Hewlett-Packard 6890 A instrument with flame ionization and thermal conductivity detectors. In the case of PE pyrolyzed in N₂ at the gas temperature of 800 °C, the major pyrolyzates included methane (25.45%), ethane (5.55%), ethylene (31.38%), propylene (7.02%), butadiene (3%), ethylacetylene (1.6%) benzene (4.44%), and hydrogen (21.61%). Ethylene was the most prominent component of the pyrolyzate gas mixture, which is consistent with the results obtained elsewhere (Goncalves et al.,⁷ Conesa et al.,¹⁰ Westerhout,¹³ Sawaguchi et al.,^{20,21} etc.). The H/C ratio in the products of pyrolysis was found to be higher (2.4) than that in the input polymer feedstock (2.0). This indicates that some carbon was removed to the condensed phase. This was indeed the case, because carbon deposits were found on the stainless-steel reactor inner walls upon post-test inspection. After examination, it was concluded that (catalytic) nanocarbon formation occurred therein. An additional experiment was performed with PE at a furnace temperature of 750 °C. The H/C ratio in the PE pyrolyzate output in this case was found to be lower, at 2.06.

In the case of PP, the major pyrolyzates included methane (33.37%), ethane (4.77%), ethylene (23.61%), propylene (7.59%), benzene (4.44%), and hydrogen (19.53%). These results differ from results obtained elsewhere,^{13,20,21} where propylene was found to have the highest mole fraction. However, those studies were conducted at 750 °C; meanwhile, the studies herein were conducted at 800 °C. Although primary pyrolysis of polyolefins tends to favor their monomers, it has been reported that higher pyrolysis temperatures¹³ and/or longer residence times²⁵ lead to higher yields of methane at the expense of ethylene and propylene. This was the case herein, as illustrated in Figure 6.

Figure 6 presents data on the pyrolyzate compositions of PE and PP in both N₂ and CO₂ atmospheres. The most notable difference is the higher hydrogen generation in the former environments (N₂), with a concomitant lower hydrocarbon generation.

The role of CO₂ on hydrogen yields in the pyrolysis gases of polyolefins can be put into perspective based on the following overall chemical reaction scheme, which is known as the reverse “water–gas shift” reaction.



This reaction is sensitive to the temperature, with the tendency to shift toward the products as the temperature increases because of Le Chatelier's principle. This is the case herein. In fact, equilibrium calculations using the STANJAN software show that, at 800 °C, this reaction alone can proceed to equimolar concentrations of CO and CO₂, if it were given sufficient time. Recent chemical kinetic studies have examined kinetic mechanisms of CO₂ addition to hydrocarbon mixtures at high temperatures. Liu et al.³⁹ studied the chemical effect of CO₂ by modeling an ethylene diffusion flame. They added CO₂ to the fuel side or to the oxidizer side with a mole fraction of 20%. They illustrated the importance of chemical kinetic effects caused by the CO₂ addition based on the elementary reactions of CO₂ + H = CO + OH and CO₂ + CH = HCO + CO. Similar conclusions were also supported by a study by Glarborg and Bentzen,⁴⁰ who examined the role of CO₂ on the formation of CO. PE and PP pyrolysis experiments performed herein under CO₂ atmospheres showed the presence of significant amounts of CO, in contrast to those under N₂ atmospheres, which showed none.

Nominally premixed flames generated from continuous feeding of PE and PP in the apparatus are shown in the photographs of Figure 7, using the Bunsen burner. In Figure 7a, a flame of natural gas is shown for comparison purposes. Panels b and c of Figure 7 show flames of PE and PP, respectively, in nitrogen carrier gas. At the estimated nearly stoichiometric conditions of this work, the natural gas and the PE flames had violet/blue tints, whereas the PP flame was blue with a faint orange surround.

As will be shown in Figure 9, the experimental natural gas flame took place at a nearly stoichiometric condition ($\phi \approx 0.99$), the particular PE flame shown in Figure 7b took place at a slightly fuel-lean condition ($\phi \approx 1.1$), and the PP flame was fuel-lean ($\phi \approx 0.90$). Stoichiometric flames have a blue hue because of chemiluminescence of CHO[•] radicals, and fuel-lean flames have a typically violet tint (see the core of the flame) because of chemiluminescence of OH[•] and CH[•] radicals, whereas fuel-rich flames have a turquoise green tint because of C₂[•] radicals.³⁷

Numerical Modeling. Predicted temperature profiles in the furnace are shown in Figures 3 and 8 and are in satisfactory agreement with the experimental results presented in Figure 3,

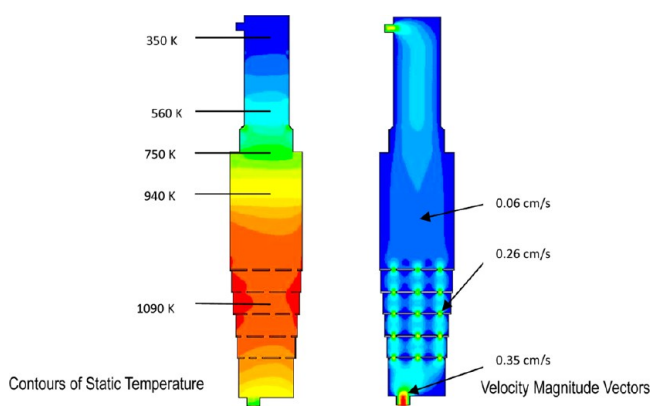


Figure 8. Results of numerical analysis (using ANSYS FLUENT), where gas velocity vectors and contours of static temperature are shown in the pyrolysis chamber.

which were obtained with a slender bare thermocouple placed along the centerline of the furnace, upon corrections for radiation (see Appendix 2). These results confirm that the temperatures present in the axial and radial directions of the heated section of the furnace are sufficient for maximum pyrolytic gasification (800 °C or 1173 K) yield from the polymer pellets. In Figure 8, the velocity vectors inside the pyrolysis chamber are also shown. High velocities at the holes of the perforated plates are predicted and are expected to enhance the polymer devolatilization rates. This ANSYS FLUENT model also predicted a high velocity at the exit of the pyrolysis chamber, which suggests that the chosen carrier gas flow rate is sufficient to force the polymer pyrolyzates through the bottom of the chamber, with no potential for recirculation back up toward the feeding system. The heating rate of the gas was calculated to be in the order of 10 °C/s.

Combustion Effluent Analysis. Once the feeding system was developed and fine-tuned to provide a continuous flame, a number of experiments were performed to quantify the effects of different temperatures and carrier gases on the levels of CO and CO₂ present in the combustion product gases. The gases were monitored by sampling the effluent of the flames and channeling the slipstream to a California Analytical Instruments dual CO–CO₂ analyzer, model 200. Given the nature of the burners used, it was not easy to accurately determine the equivalence ratio of their nominally premixed flames based on the amount of reactants. Hence, the equivalence ratio was estimated on the basis of the measured CO and CO₂ combustion products. To achieve this, the partial pressures of the combustion products of pyrolyzate gases were calculated using the chemical equilibrium code STANJAN.²⁶ For this calculation, the pyrolyzate gas mixture composition, documented in Figure 6, was input to the code as reactants (along with the respective carrier gas) and the molar amount of the major combustion products (O₂, N₂, CO, CO₂, H₂O, NO, and NO₂) was computed. The calculation was run over several iterations, with the O₂ mole fraction in the reactants altered to produce a range of CO₂/CO ratios. These ratios are plotted against the experimentally measured results for comparison purposes in Figure 9. It should be mentioned that data points were obtained at two set-point temperatures of the pyrolytic gasification furnace: 900 and 950 °C. Experiments were run for 20 min and were repeated at least in triplicate; average mole fractions and standard deviations are shown in Figure 9. The scatter in the experimental data is attributed to fluctuations in the feeding rate, as documented in Figure 4. For comparison purposes, experimental CO₂/CO data obtained burning natural gas in the same burner (see Figure 7) are also included in the same figure.

On the basis of the predictions of the chemical equilibrium code STANJAN, it can be inferred that, in most cases, combustion took place in the broad neighborhood of stoichiometry. Moreover, there was some scatter in the emission data, which may be attributed to some unsteadiness in the pellet feeding and devolatilization as well as to mild fluctuations of the air supply to the Bunsen burner under the operating fume hood. Surprisingly, similar fluctuations in the emission data were also observed for the case of the natural gas flames, suggesting that the latter mechanism was a significant contributor to this scatter. It may also be observed from these figures that all fuels resulted in comparable CO₂/CO ratios, under the conditions of this work, confirming that the

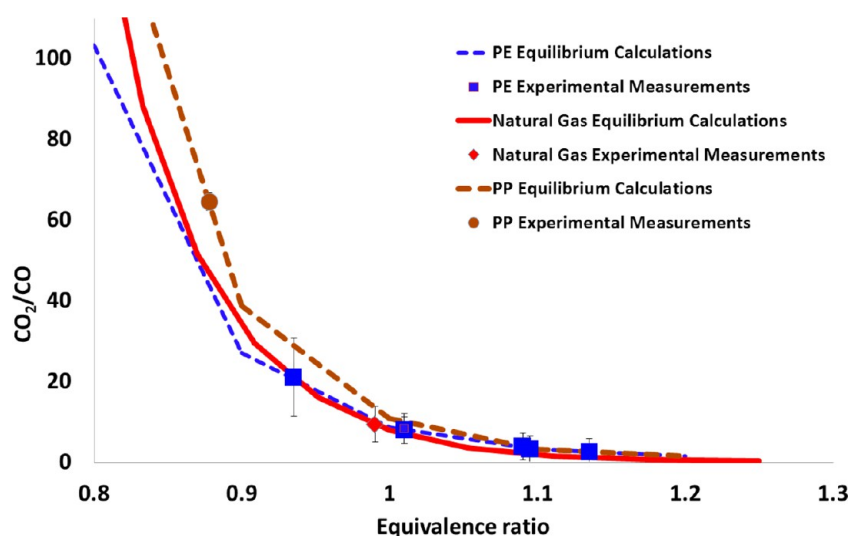


Figure 9. Experimentally determined CO_2/CO versus calculated equivalence ratio, ϕ , at various implemented pyrolytic gasification reactor operating conditions. N_2 was used as the carrier gas in these experiments.

effectiveness of combustion of the gaseous pyrolyzates of post-consumer polyolefins is akin to that of natural gas.

On the Comparative Emissions from Indirect and Direct Combustion of Polyolefins. Indirect combustion of polyolefins, using the scheme implemented herein of first gasifying the polymers and then homogeneously burning their pyrolyzates with air, is much less polluting than direct combustion of the same polymers. The former mode of combustion employs premixed flames, where the fuel/air equivalence ratio [the fuel/air equivalence ratio is defined as $\phi = (m_{\text{fuel}}/m_{\text{air}})_{\text{actual}} / (m_{\text{fuel}}/m_{\text{air}})_{\text{stoichiometric}}$] can be readily controlled, whereas the latter mode of combustion results in diffusion flames forming around burning polymer chunks, where the fuel/air equivalence ratio cannot be controlled. Control of the equivalence ratio to an appropriate substoichiometric level (fuel-lean) can lead to low emissions. Thus, such fuel-lean premixed combustion may be characterized as “clean”. Past results obtained in this laboratory documented that indirect combustion of polyolefins and other polymers minimized emissions of toxic pollutants. Gonçalves et al.⁷ reported that both the cumulative and individual component yields of health-hazardous PAHs as well as the particulate yields (mostly soot and tars) from indirect combustion of pulverized PE in a drop-tube furnace were more than 10 times smaller than the corresponding yields from direct combustion of PE in a variety of experimental setups in this laboratory, operated under diverse experimental conditions^{27–36} (see Figure 6 therein). CO yields from the indirect combustion of PE also appeared to be lower than those from direct combustion of this polymer at comparable equivalent ratios. Finally, CO_2 yields from indirect combustion of PE in the case of Gonçalves et al.⁷ and in the case herein as well as in the case of ethylene combustion³⁶ were higher than those from direct batch combustion of PE, reported by Wang et al.,³⁴ which is indicative of more complete combustion.

On the Replacement of Nitrogen Background Carrier Gas with Carbon Dioxide. Substitution of background N_2 gas with CO_2 was very well-tolerated by the flame, producing no discernible differences. As expected, because CO_2 was added to the pyrolytic gasifier input, the amount of CO_2 in the effluent was also higher than in experiments where N_2 was used

as the carrier inert gas (see Table 1). Small variations in CO concentrations may be attributed to fluctuations in the polymer

Table 1. Average Mole Fractions of Carbon Dioxide and Carbon Monoxide in the Combustion Effluent of PE, along with Computed Standard Deviations

	CO_2 carrier gas	N_2 carrier gas
	$T_{\text{set point}} = 900\text{ }^\circ\text{C}$	$T_{\text{set point}} = 900\text{ }^\circ\text{C}$
CO_2 (%)	14.2 ± 1.04	11.1 ± 0.7
CO (%)	0.6 ± 0.1	1.5 ± 0.5

pellet feeding rate. The implication of substitution of the nitrogen background inert gas with carbon dioxide in the pyrolytic gasifier may prove to be important in the economics of an industrial-scale application. The use of N_2 as a carrier gas requires the procurement, maintenance, and servicing of on-site N_2 gas storage. This is costly, takes up space, and diverts valuable resources to maintaining such a system. CO_2 is a byproduct of combustion, and devising a system to capture CO_2 produced from combustion gases to be used as a carrier gas in the system will present significant cost and resource savings, because CO_2 is produced at no additional cost and diminishing the supply of it is not a factor, as with storing bottled N_2 on site.

Conversion of Post-consumer Plastics To Electricity the Proof of Concept. A technical goal of this project has been to produce a continuous flame with sufficient energy to run the miniature steam engine and produce direct current (DC) electricity through a generator and to eventually turn on a light bulb, shown in Figure 10. As mentioned before, a polymer mass feeding rate of 1 g/min produced a flame that was more than sufficient to generate steam and run the miniature steam engine at a high speed. The flame burned with bright bluish colors (see Figure 10). The steam engine system was able to sustain a boiler pressure of 1 bar and operate consistently at 1800 rpm for the duration of an experiment, which was set to 20 min. This operational speed was sufficient to use the on-board generator to produce a small electric current to illuminate the miniature light bulb. This demonstrated the concept that waste plastics can be used to produce

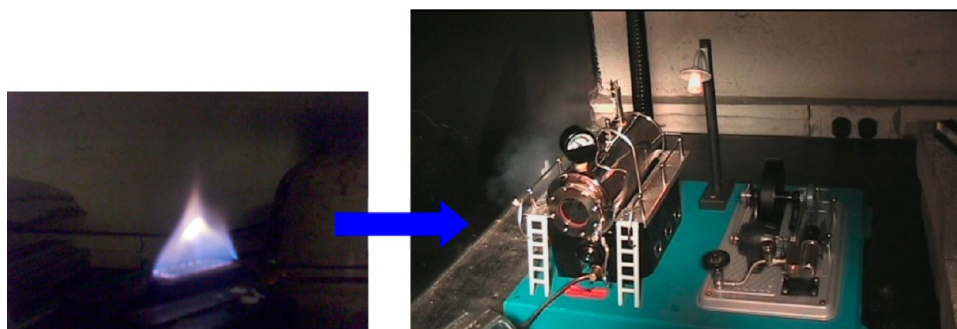


Figure 10. Miniature steam engine in action powered by combustion of pyrolyzates of post-consumer PE in a small burner. The coupled electricity generator powers the light bulb.

gaseous fuels with high energy content and, in turn, can reliably generate useful work in the form of electricity (see Figure 10).

CONCLUSION

A laboratory-scale system was designed and developed for experimentation. This system is able to pyrolyze pelletized post-consumer (waste) plastics. It was seen that the composition of the pyrolyzates were mostly hydrogen, methane, and ethylene. These light hydrocarbons can be easily premixed with air in such a way that the amount of air can be adjusted to reach a desired equivalence ratio.

Power generation was demonstrated with a model steam engine, and it was shown that the system was stable and capable of generating electricity for long periods of time (20 min tests were conducted herein). Both CO_2 and N_2 were used as background carrier gases for polyolefin pyrolysis, and their effects on the pyrolyzate gas compositions were explored. The amounts of light hydrocarbons in the pyrolyzate effluents at the presence of both background gases were similar. The main difference was that a lower amount of hydrogen was detected in the CO_2 environment and was attributed to water–gas shift reactions. Future considerations for the system include designing a self-sustaining system, in which the electric heater would be replaced by a gas burner, where a fraction of the pyrolyzates would be burned to supply heat to the pyrolytic gasifier.

APPENDIX 1: CALCULATION OF THE ENERGY INPUT REQUIRED FOR PYROLYSIS OF POLYOLEFINS, $E_{\text{PYROLYSIS}}$

The energy required for pyrolysis of PE and PP at 500°C has been reported by Gupta and co-workers to be 351 and 911 kJ/kg, respectively.³ At the higher temperature of 950°C , the corresponding energy requirement per unit mass of feedstock ($Q_{\text{pyrolysis}}$) is calculated using eq 1.

$$E_{\text{pyrolysis}} = E_{\text{pyrolysis initialization}} + C_p \Delta \dot{m} \quad (1)$$

with the assumption that the heat capacity changes linearly with the temperature. Performing interpolations:

$$T_{\text{avg,PE}} = \frac{500 + 950}{2} + 273 = 998 \text{ K} \quad (2)$$

$$T_{\text{avg,PP}} = \frac{496 + 950}{2} + 273 = 996 \text{ K} \quad (3)$$

based on the gaseous properties from the National Institute of Standards and Technology (NIST) database

$$C_{p,\text{PE}-T_{998}} \cong 3.35 \text{ kJ kg}^{-1} \text{ K}^{-1}$$

$$C_{p,\text{PP}-T_{996}} \approx 3.44 \text{ kJ kg}^{-1} \text{ K}^{-1}$$

Substituting these two values into eq 1 yields the following pyrolysis energy:

$$E_{\text{PE-pyrolysis}} = 351 + 3.35(950 - 500) = 1859 \text{ kJ/kg} \quad (4)$$

$$E_{\text{PP-pyrolysis}} = 911 + 3.34(950 - 500) = 2414 \text{ kJ/kg} \quad (5)$$

Therefore, the energy requirement needed to pyrolyze the polyolefins, $E_{\text{polyolefin-pyrolysis}}$ is in the range of 1.8–2.4 MJ/kg.

APPENDIX 2: THERMOCOUPLE TEMPERATURE MEASUREMENT CORRECTION FOR RADIATION EFFECTS

The temperature at different elevations of the pyrolysis chamber was measured with a bare thermocouple. These readings need to be corrected to exclude the furnace wall radiation effects. This correction is based on an energy balance on the thermocouple bead.

$$\rho C_p V \frac{dT_b}{dt} = \dot{Q}_{\text{convection}} + \dot{Q}_{\text{radiation}} \quad (6)$$

It is assumed that the bead of the thermocouple is in thermal equilibrium with its surroundings (steady state). A k-type OMEGA thermocouple was used for these measurements, and the diameter of the bead was measured to be $250 \mu\text{m}$. By considering steady-state conditions, Eq 6 becomes

$$\dot{Q}_{\text{convection}} + \dot{Q}_{\text{radiation}} = 0 \quad (7)$$

Convection and radiation terms are determined from

$$\dot{Q}_{\text{convection}} = h A_b (T_{\text{gas}} - T_b) \quad (8)$$

$$\dot{Q}_{\text{radiation}} = \epsilon_b \sigma A_b (T_{\text{wall}}^4 - T_b^4) \quad (9)$$

where A_b is the area of the bead and T_{gas} and T_b are temperatures of the gas and bead, respectively. The heat-transfer coefficient h can be calculated from eqs 10 and 11 by considering the bead to be a spherical object.

$$Nu = \frac{hD}{k} = 2 + \frac{0.589 Ra_D^{1/4}}{\left[1 + \left(\frac{0.469}{Pr} \right)^{9/16} \right]^{4/9}} \quad (10)$$

$$Ra_D = \frac{g\beta(T_b - T_{\text{gas}})D^3}{\nu^2} \times Pr \quad (11)$$

The Nusselt number, Nu , represents the ratio of the convection to conduction heat interactions across the fluid layer. The Rayleigh number, Ra , is dimensionless and is being used for calculating natural convection heat interactions. The Prandtl number, Pr , is also another dimensionless number that depicts the velocity and thermal boundary layer thicknesses relatively.

The Nusselt number that is calculated on the basis of the above expression is valid for $Ra_D < 10^{11}$ and $Pr > 0.7$.

Finally, eq 9 becomes

$$hA_b(T_{\text{gas}} - T_b) + \varepsilon_b \sigma A_b(T_{\text{wall}}^4 - T_b^4) = 0 \quad (12)$$

It needs to be mentioned that, for obtaining the convection coefficient, we need to have the thermal conductivity of the gas. For calculation of the thermal conductivity, there are relations that can be used, and because these relations are based on the gas temperature, it is needed to first assume a value for the gas temperature and then solve eq 12 by trial and error.

Table A2.1. Comparison between Corrected and Uncorrected Temperature Readings

measured temperature with thermocouple (°C)	corrected gas temperature (°C)
390	371
610	598
650	639
690	681
790	784
830	825
840	836
855	851
855	851

■ APPENDIX 3: BASIC ECONOMIC ANALYSIS

Market prices for recycled post-consumer plastics in 2012 are in the range of \$0.05–0.5/kg, depending upon cleanliness, sorting, separation, pelletization, etc. Given that the energy content of polyolefins is in the neighborhood of 45 MJ/kg, then the specific price range of recycled plastics per energy content is in the range of \$1–11/GJ. This is analogous to the specific price range of natural gas, which, in the past 10 years, fluctuated between \$2 and \$14/GJ. Hence, for recycled plastics to have a competitive advantage as a fuel, their price should stay as low as

Table A3.2

polymer fed	kg/h	1000
carrier gas required	L/kg of polymer	250
carrier gas feed (nitrogen)	L/h	250000
hours/shift	h	8
shifts/day	quantity	2
uptime	75%	0.75
hours/day	h	12
maintenance rate	\$/h	50
daily maintenance cost	\$/day	600
labor rate	\$/h	50
daily labor cost	\$/day	600
daily polymer feed	kg/day	12000
daily carrier gas use	L/day	3000000
energy content LDPE	kJ/kg	46300
pyrolysis energy LDPE	kJ/kg (10% of total energy content, per Appendix 2 calculations)	4630
energy input	kJ/day	555600000
energy used to pyrolyze	kJ/day (10% of total input)	55560000
energy available for recovery	kJ/day	500040000
wholesale energy price	New England (http://www.eia.gov/electricity/wholesale/), \$/kWh	0.056
recovered energy efficiency factor	35%, typical Rankine cycle power plant	0.35
recovered energy	kJ/day	175014000
recovered energy	kWh/day	48615
recovered energy value per day	\$/day	2722.44
cost of carrier gas	\$/unit	0.00028
daily cost of carrier gas	\$/day	840

possible, preferably as close as possible to the lowest price, i.e., in the vicinity of \$1/GJ. Therefore, it is recommended that a power plant is built in the vicinity of a recycling center, to avoid transportation costs and other handling costs and maximize profits. A simple economic model was constructed to perform calculations for a simplified setup. Some general assumptions were made on manning (two 8 h shifts per day) and maintenance costs of \$600/day as well as efficiency for the electric power generation. The running costs are assumed to be \$50/h for labor with 16 h per day of runtime. To add an extra measure of conservatism to the estimate, an overall system uptime of 75% is assumed. The system would need to process in excess of 638 kg/h to turn a profit. Table A3.1 details the results of the model being run for the cases of 100–1000 kg/h

Table A3.1

feed rate (kg/h)	income (\$/day)	income (\$/kg)	expenditures (\$/day)	expenditures (\$/kg)	net cashflow (\$/day)	net cashflow (\$/kg)
100	272	0.227	1284	1.070	1012	0.843
200	544	0.227	1368	0.570	824	0.343
300	817	0.227	1452	0.403	635	0.176
400	1089	0.227	1536	0.320	447	0.093
500	1361	0.227	1620	0.270	259	0.043
600	1633	0.227	1704	0.237	71	0.010
700	1906	0.227	1788	0.213	118	0.014
800	2178	0.227	1872	0.195	306	0.032
900	2450	0.227	1956	0.181	494	0.046
1000	2722	0.227	2040	0.170	682	0.057

feed rate. The feed rate was varied, and the resulting outputs for both income and expenditures are calculated on a per kilogram and per day basis. The net income per kilogram of plastic is constant, and the running costs are spread out among the feed rate, thus resulting in a diminishing running cost per kilogram as feed rate increases. As mentioned above, the break-even point is 638 kg/h. At higher feed rates than this, the running cost becomes spread more evenly and the per unit mass (kg) running costs become less than the per kilogram income (see Table A3.2).

AUTHOR INFORMATION

Corresponding Author

*E-mail: y.levendis@neu.edu.

Notes

The authors declare no competing financial interest.

ACKNOWLEDGMENTS

The authors thank Massachusetts Clean Energy Center (MassCEC) for financial support through the MassCEC Catalyst Award Program and the Garlock Sealing Technologies for the donation of high-temperature gaskets. The authors also acknowledge Christopher Flanagan, Anna Craver, Brittne Lynn, Mason Riley, and Katherine Dixon for technical assistance in the design and development of the hardware.

REFERENCES

- (1) United States Environmental Protection Agency (U.S. EPA). *Wastes—Resource Conservation—Common Wastes and Materials*; U.S. EPA: Washington, D.C., 2012; <http://www.epa.gov/osw/conservation/materials/plastics.htm> (accessed April 29, 2013).
- (2) United States Environmental Protection Agency (U.S. EPA). *Municipal Solid Waste (MSW) in the United States: Facts and Figures*; U.S. EPA: Washington, D.C., 2010; <http://www.epa.gov/osw/nonhaz/municipal/msw99.htm> (accessed April 29, 2013).
- (3) Jinno, D.; Gupta, A. K.; Yoshikawa, K. *Environ. Eng. Sci.* **2004**, *21* (1), 65–72.
- (4) Caponero, J.; Tenório, J. A. S.; Levendis, Y. A.; Carlson, J. B. *Combust. Sci. Technol.* **2005**, *177* (2), 347–381.
- (5) Ergut, A.; Levendis, Y. A.; Carlson, J. *Fuel* **2007**, *86* (12–13), 1789–1799.
- (6) Gonçalves, C. K.; Tenório, J. A. S.; Levendis, Y. A.; Carlson, J. B. *Energy Fuels* **2007**, *22* (1), 354–362.
- (7) Gonçalves, C. K.; Tenório, J. A. S.; Levendis, Y. A.; Carlson, J. B. *Energy Fuels* **2007**, *22* (1), 372–381.
- (8) DiNunno, P. J. *SFPE Handbook of Fire Protection Engineering*; National Fire Protection Association: Quincy, MA, 1988.
- (9) Sørum, L.; Grønli, M. G.; Hustad, J. E. *Fuel* **2001**, *80* (9), 1217–1227.
- (10) Conesa, J. A.; Font, R.; Marcilla, A.; Garcia, A. N. *Energy Fuels* **1994**, *8* (6), 1238–1246.
- (11) Scott, D. S.; Czernik, S. R.; Piskorz, J.; Radlein, D. S. A. G. *Energy Fuels* **1990**, *4* (4), 407–411.
- (12) Kaminsky, W. *Resour. Recovery Conserv.* **1980**, *5* (3), 205–216.
- (13) Westerhout, R. W. J.; Waanders, J.; Kuipers, J. A. M.; van Swaaij, W. P. M. *Ind. Eng. Chem. Res.* **1998**, *37* (6), 2293–2300.
- (14) Mastral, J. F.; Berruete, C.; Ceamanos, J. *Energy Fuels* **2006**, *20* (4), 1365–1371.
- (15) Lee, J. W.; Yu, T. U.; Lee, J. W.; Moon, J. H.; Jeong, H. J.; Park, S. S.; Yang, W.; Lee, U. D. *Energy Fuels* **2013**, *27* (4), 2092–2098.
- (16) Zhuo, C.; Hall, B.; Richter, H.; Levendis, Y. *Carbon* **2010**, *48* (14), 4024–4034.
- (17) Costa, P. A.; Pinto, F. J.; Ramos, A. M.; Gulyurtlu, I. K.; Cabrita, I. A.; Bernardo, M. S. *Energy Fuels* **2007**, *21* (5), 2489–2498.
- (18) Mastral, F. J.; Esperanza, E.; García, P.; Juste, M. J. *Anal. Appl. Pyrolysis* **2002**, *63* (1), 1–15.
- (19) Faravelli, T.; Bozzano, G.; Scassa, C.; Perego, M.; Fabini, S.; Ranzi, E.; Dente, M. J. *Anal. Appl. Pyrolysis* **1999**, *52* (1), 87–103.
- (20) Sawaguchi, T.; Suzuki, K.; Kuroki, T.; Ikemura, T. *J. Appl. Polym. Sci.* **1981**, *26* (4), 1267–1274.
- (21) Sawaguchi, T.; Inami, T.; Kuroki, T.; Ikemura, T. *Ind. Eng. Chem. Process Des. Dev.* **1980**, *19* (1), 174–179.
- (22) Yamada, H.; Mori, H.; Tagawa, T. *J. Ind. Eng. Chem.* **2010**, *16* (1), 7–9.
- (23) Kondo, S.; Takizawa, K.; Takahashi, A.; Tokuhashi, K. *Fire Saf. J.* **2006**, *41* (5), 406–417.
- (24) Talebi Anaraki, S. Waste to energy conversion by stepwise liquefaction, gasification and “clean combustion” of pelletized waste polyethylene for electric power generation - in a miniature steam engine. Master's Thesis, Northeastern University, Boston, MA, 2012.
- (25) Norinaga, K.; Deutschmann, O.; Hüttinger, K. J. *Carbon* **2006**, *44* (9), 1790–1800.
- (26) Dandy, D. S. *STANJAN Chemical Equilibrium Calculation*; Bioanalytical Microfluidics Program, Department of Chemical and Biological Engineering, Colorado State University: Fort Collins, CO, 2013; <http://navier.engr.colostate.edu/~dandy/code/code-4/>
- (27) Green, A. E. S.; Sadrameli, S. M. *J. Anal. Appl. Pyrolysis* **2004**, *72* (2), 329–335.
- (28) Wheatley, L.; Levendis, Y. A.; Vouros, P. *Environ. Sci. Technol.* **1993**, *27* (13), 2885–2895.
- (29) Panagiotou, T.; Levendis, Y. A.; Carlson, J.; Vouros, P. *Symp. (Int.) Combust., [Proc.]* **1996**, *26* (2), 2421–2430.
- (30) Panagiotou, T.; Levendis, Y. A.; Carlson, J.; Dunayevskiy, Y. M.; Vouros, P. *Combust. Sci. Technol.* **1996**, *116* (1–6), 91–128.
- (31) Shemwell, B. E.; Levendis, Y. A. *J. Air Waste Manage. Assoc.* **2000**, *50* (1), 94–102.
- (32) Wang, J.; Levendis, Y. A.; Richter, H.; Howard, J. B.; Carlson, J. *Environ. Sci. Technol.* **2001**, *35* (17), 3541–3552.
- (33) Wang, J.; Richter, H.; Howard, J. B.; Levendis, Y. A.; Carlson, J. *Environ. Sci. Technol.* **2002**, *36* (4), 797–808.
- (34) Wang, Z.; Wang, J.; Richter, H.; Howard, J. B.; Carlson, J.; Levendis, Y. A. *Energy Fuels* **2003**, *17* (4), 999–1013.
- (35) Wang, Z.; Richter, H.; Howard, J. B.; Jordan, J.; Carlson, J.; Levendis, Y. A. *Ind. Eng. Chem. Res.* **2003**, *43* (12), 2873–2886.
- (36) Hall, B.; Zhuo, C.; Levendis, Y. A.; Richter, H. *Carbon* **2011**, *49* (11), 3412–3423.
- (37) Hilliard, J. Internal combustion engines, lecture notes; University of Michigan, Ann Arbor, MI, 1982.
- (38) Flanagan, C.; Craver, A.; Lynn, B.; Riley, M.; Dixon, K.; Zhuo, C.; Levendis, Y. Method and device for fuel and power generation by clean combustion of organic waste material. WO 2012075499 A1, 2012.
- (39) Liu, F.; Guo, H.; Smallwood, G. J.; Gulder, O. L. *Combust. Flame* **2001**, *125* (1–2), 778–787.
- (40) Glarborg, P.; Bentzen, L. L. B. *Energy Fuels* **2008**, *22* (1), 291–296.